

Impact of treatment time on single annealing thermal cycle performed on Ti-6Al-4V Titanium alloy specimens obtained using LPBF technology

E. Ferrari, S. Gaiani, M. Gozzi, M. Lassinantti Gualtieri, F. Mantovani,
G. Ponzoni, P. Veronesi

Additive manufacturing has become a prominent solution for producing intricate components with complex geometries. Titanium alloy Ti-6Al-4V is widely used in additive manufacturing due to its excellent mechanical properties, low density, and corrosion resistance. However, residual stresses generated during the laser powder bed fusion (LPBF) process require specific heat treatments. This research aims to determine the optimal temperature-time parameters of thermal cycles able to reduce residual stresses while achieving desired microstructural conditions. Previous research investigated the impact of heat treatments at different temperatures, with annealing at 800°C and 835°C for 2 hours resulting in the best mechanical properties. The samples treated at 800°C exhibited increased ductility due to the onset transformation of α' to $\alpha + \beta$. The samples treated at 835°C showed a favorable balance between mechanical properties and plasticity. This study expands on the previous research by comparing different treatment times at optimal temperatures and investigating their effect on average mechanical properties and their variance. Complete mechanical and microstructural characterization, including XRD analysis, was conducted on the treated samples.

KEYWORDS: ADDITIVE MANUFACTURING, TI-6AL-4V, STRESS RELIEF, HEAT TREATMENT STRATEGIES, MICROSTRUCTURE

INTRODUCTION

Additive manufacturing techniques, such as laser powder bed fusion (LPBF), have revolutionized the production of components by providing remarkable mechanical properties. The rapid solidification rates achieved during the LPBF process contribute to these properties. However, the rapid and repeated cooling involved in the process results in high levels of residual stresses in the printed parts, which can lead to distortions and surface defects upon removal from the building platform [1]. To optimize the microstructure and mechanical properties of materials, it is common practice to postprocess almost all additive manufacturing parts, by proper heat treatments, before their removal from the building platform.

Extensive research has been conducted on postprocess heat treatments of Ti-6Al-4V components manufactured using LPBF technology [2]. The objective of these studies is to identify optimal heat treatment cycles that

E. Ferrari, M. Gozzi

Veca SpA, Italy
elisa.ferrari@veca.it
marica.gozzi@veca.it

S. Gaiani

V System, srl. Italy
silvia.gaiani@vsystem.it

M. Lassinantti Gualtieri, P. Veronesi

Università degli Studi di Modena e Reggio, Italy
magdalena.gualtieri@unimore.it
paolo.veronesi@unimore.it

F. Mantovani, G. Ponzoni

AMT srl, Italy
flavia.mantovani@amt-srl.com
greta.ponzoni@amt-srl.com

effectively eliminate residual stresses and achieve a proper microstructural balance. The generation of residual stresses is attributed to the expansion and contraction interactions between layers induced by the large thermal gradients inherent in the LPBF process, where a laser spot scans the surface and induces localized melting.

The typical microstructure of Ti-6Al-4V alloys obtained by LPBF consists of an extremely fine acicular martensitic structure known as the alpha prime (α') phase [3]. This microstructure is a result of the extremely fast heating and cooling rates typical of the LPBF process. Additionally, the as-built microstructure of LPBF components usually consists of an acicular martensitic phase within columnar β grains, exhibiting a pronounced orientation along the building direction [4]. The inclination of the martensitic needles at an angle of approximately 45 degrees with respect to the manufacturing direction is a characteristic feature [5]. These microstructural characteristics contribute to the high yield strength (>1000 MPa), high ultimate tensile strength, and elongations in the range of 7-10% observed in LPBF Ti-6Al-4V components [6]. It should be noted that the reduction in the ductility of parts is not necessarily observed throughout the entire thickness of the built part but rather depends on its shape, scanning strategy, and other factors. A literature review indicates that while the yield and tensile strengths of LPBF components are significantly greater than the ASTM specifications for the biomedical or aerospace sector, the reported values for tensile strain often fall below the minimum needed.

The width of the α or α' phase plays a significant role in determining the strength of LPBF-fabricated lamellar structures. The effective slip length for dislocation is limited to the individual martensite width rather than the α colony size [7]; hence, controlling the dimension of the alpha phases is crucial for achieving the desired strength. Consequently, postprocessing heat treatments are designed not only to eliminate residual stress but also to control the size of the alpha phases, as a Hall-Petch relationship exists between the width of the alpha phases and the strength of the material.

Numerous studies have been conducted to investigate the

effect of different postprocess heat treatment strategies on the mechanical properties and microstructural evolution of LPBF Ti6Al4V alloy components. These studies have explored various temperatures, holding times, and cooling rates to optimize the process parameters and achieve excellent mechanical properties and good ductility. However, the decomposition kinetics of alpha prime (α') martensite and the precise optimization of process parameters require further research and deeper insights [8][9][10][11][12].

In the industrial manufacturing of LPBF Ti6Al4V components, post-heat treatments also aim to minimize the variability of the mechanical properties within the same build [13]. As a matter of fact, a more robust postprocess treatment would also help designers in selecting the proper minimum expected mechanical properties. LPBF processes are influenced by various factors that can lead to deviations in mechanical properties, even within the same build [14]. These deviations can be reduced through carefully designed heat treatments that induce microstructural modifications. Hot Isostatic Pressing (HIP) [15] is known to help decreasing the porosity of parts and is considered as a reliable process for improving the tensile performance and modifying the microstructure at elevated temperatures [16]. However, HIP alters the microstructure by inducing coarse lamellar α and β formation, resulting in a negative impact on strength despite reducing porosity and increasing elongation [17].

In a previous work by the authors [30] it was demonstrated that by applying a proper post-heat treatment for LPBF Ti6Al4V parts, the exceptional mechanical properties associated with the fine microstructure typical of LPBF can be preserved, while minimizing the variability of the mechanical properties within the same build. In that work, comprehensive analyses were performed to better understand the effects of post-heat treatments on LPBF Ti6Al4V components. It was found that the sub beta-transus heat treatment at 830°C for 2 hours retained the excellent mechanical properties of the as-built samples while increasing elongation and reducing variance among samples from different locations within the same building. The study also investigated the impact of temperature on the mechanical properties, noting a modification in

the mechanical properties and elongation and, more importantly, presenting a lower variance within samples belonging to the same build but with a different part location. This study aims to select an annealing condition at this temperature able to provide high strength, good ductility, and a uniform distribution of characteristics across the entire printing area.

This new study aims to analyze the influence of heat treatment time, using as a reference the two best-performing treatments from the previous research [30], namely, single annealing cycles at 800°C and 835°C for two hours. These two treatments will be compared with thermal cycles performed at the same temperature but with a doubled treatment time, i.e., 4 hours.

This study serves to thoroughly understand how to optimize the heat treatment process to achieve a more robust result and achieving the maximum material properties despite possible bias introduced for instance by part location in the building chamber or different LPBF units.

MATERIALS AND METHODS

Samples

For the present study, two samples with different shapes (circular and rectangular cross section) were manufactured using 3 different LPBF units of the same brand. Specimens extracted from different positions of the builds were subjected to various heat treatment cycles (C1-C4, described later in section 2.2.).

The cylindrical samples had a diameter of 10 mm and a height of 120 mm whereas the rectangular samples had the dimensions 20x13x3.5 mm. Both types of samples were built in the vertical direction.

For the thermal cycles C1 and C2, sets of 30 cylindrical samples were built using an EOS M290 LPBF unit. Six different part locations on the building platform were sampled: the corners at a 10 mm distance from the platform edges, and in the central position at two symmetrical positions spaced 100 mm along the y direction.

For the thermal cycle C3, sets of 3 samples with rectangular cross section were built using a EOS SI2051 LPBF unit. For C4 sets of 20 cylindrical samples, were manufactured using an EOS SI3826 LPBF unit. All builds were accomplished using a virgin commercial Ti-6Al-4V powder from ELI EOS GmbH Electro Optical Systems.

The same process parameters were used in all units, namely:

- Average powder grain size: D90 (48–51 μm);
- Source power: 340 W (single laser source);
- Printing speed: 1250 mm/s;
- Spot size: 80 μm ;
- Layer thickness 50 μm

Heat treatment strategy

In the present study, three different post-process vacuum heat treatment strategies were considered and investigated (Table 1).

Tab.1 - Heat treatment cycles used in this paper.

Heat Treatment Cycles				
CYCLE	TEMPERATURE	TIME	COOLING	OVEN UNIT
C1	800°C	2 h	Constant cooling rate 11°C/min + Ar flux	Vacuum Oven
C2	800°C	4 h	Constant cooling rate 11°C/min + Ar flux	Vacuum Oven
C3	835°C	2h	Constant cooling rate 11°C/min + Ar flux	Vacuum Oven
C4	835°C	4h	Constant cooling rate 11°C/min + Ar flux	Vacuum Oven

This treatment strategy is a single annealing thermal cycle. The thermal cycles were performed at two different temperatures, above 780 °C, but always below β transus transition temperature to avoid excessive grain growth. Operating at these temperatures, an α prime transformation is expected and will theoretically be more relevant as

temperature increases. The expected advantages are an increased homogeneity of mechanical response and increased elongation at break and ductility, while the higher temperature could have a detrimental effect on the peak mechanical properties (UTS and Rp0.2); In order to have a better understanding of the impact of

different heat treatment strategies on Ti-6Al-4V alloy, some samples in the "as built" condition have also been tested as a reference of initial basic properties that can be obtained directly via the LPBF process.

All heat treatments have been conducted on a TAV vacuum unit H6 S, having chamber dimensions of 600 x 600 x 900 mm and maximum Ar pressure during cooling of 11.5 bar. Heat treatment has been performed using a charge thermocouple, i.e., a thermocouple positioned in contact with one of the samples, where a 1 mm diameter hole, 20 mm deep, had been drilled to fix the K-type thermocouple in place.

Type of analyses

The samples heat treated with the different strategies discussed in Section 2.2 were characterized by means of micro-hardness test, tensile tests, microstructural examination with optical microscope, and microstructural phase determination with X-ray Diffraction (XRD).

Tensile tests were performed in accordance with standard EN ISO 6892-1:2016 and using fully machined cylindrical specimens with $L_0 = 20$ mm and $D_0 = 4$ mm. The tests were performed using the constant strain rate method (A1 mode with closed-loop control). Five tests at room temperature were performed for each set of samples subjected to the heat treatment strategy shown in Table 1, using a hydraulic universal press Instron 5982 with 100 kN maximum load;

For optical micrographic analysis, samples were mechanically grounded using SiC grinding paper and then polished with colloidal silica (0.04 μm) and hydrogen peroxide (30%). Kroll reagent (5 mL HNO_3 ; 10 mL HF; 85 mL H_2O) was used as an etchant. Samples were then analyzed using a Nikon Eclipse LV150-NL optical microscope and fluoride lenses. Higher magnification observations were performed using scanning electron

microscopy (ESEM Quanta-200 Fei, Hillsboro, OR, USA, and SEM Nova NanoSEM 450-FEI).

X-ray Diffraction (XRD) data were collected in Bragg-Brentano configuration using an X'Pert PRO multi-purpose diffractometer (PANalytical, Almelo, The Netherlands) equipped with a Real-Time Multiple Strip (RTMS) detector. The Cu-K radiation emitted from the X-ray tube at 40 kV and 40 mA passed through fixed divergence and anti-scatter slits (both 0.5°) as well as a soller slit (0.04 rad) before interacting with the sample. The beam width was adjusted using a mask of 10 mm. The diffracted beam pathway included a Ni filter, a soller slit (0.04 rad), and an anti-scatter blade (5 mm). Data were collected in the angular range 10–120° 2θ using a step size of 0.0167° and 40 s/step. Phase identification was accomplished with the aid of the X'Pert Highscore plus software (2.0, PANalytical B.V., Almelo, The Netherlands) implemented with the PDF2 database.

Microhardness tests were accomplished using a Wilson VH1202 microhardness tester with a load of 0.5 kg. The impressions were made with a dwell time of 12 seconds. Before measurements, samples were subjected to metallographic preparation mounted using a Struers model Citopress-5 and polished using a Struers model Laboforce 100 lapping machine. Five tests at room temperature were performed for each set of samples subjected to the heat treatment strategy shown in Table 1

RESULT AND DISCUSSION

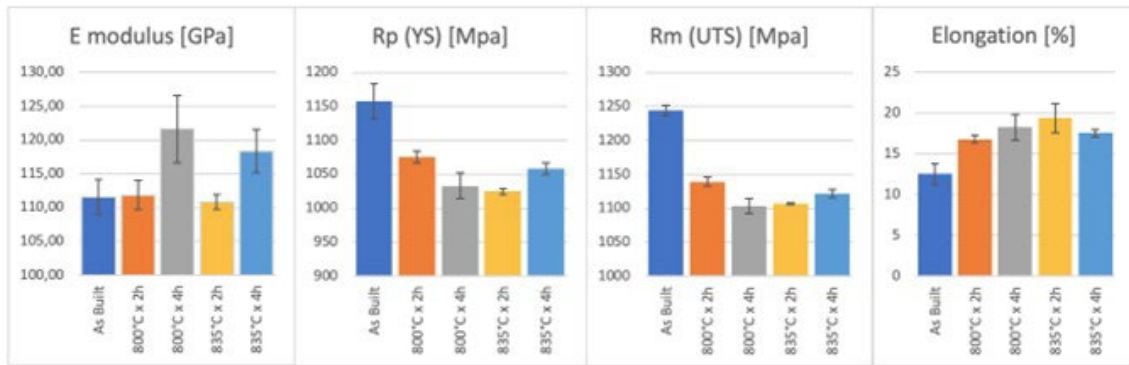
In this section, a concise description of the experimental results and their interpretation will be provided.

Tensile test result

The results of tensile tests performed on samples along the growth direction (Z direction) are summarized in Table 2.

Tab.2 - Tensile test result and graphic.

Tensile test result				
CYCLE	E (GPa)	Rp 0,2 (MPa)	UTS (MPa)	Elongation (%)
As Built	111.62 ± 2.58	1157.59 ± 25.56	1244.26 ± 7.81	12.55 ± 1.26
C1 (800°Cx2h)	111.85 ± 2.14	1075.40 ± 8.18	1139.45 ± 6.67	16.79 ± 0.44
C2 (800°Cx4h)	121.64 ± 4.95	1033.16 ± 19.20	1103.17 ± 11.32	18.28 ± 1.58
C3 (835°Cx2h)	110.83 ± 1.09	1025.01 ± 4.46	1107.47 ± 1.43	19.36 ± 1.77
C4 (835°Cx4h)	118.34 ± 3.18	1058.51 ± 8,92	1121.87 ± 6.19	17.55 ± 0,47



The high tensile strength and low ductility of as built samples is ascribable to their complete martensitic α' microstructure, as opposed to the predominant $\alpha + \beta$ typical of annealing-treated samples. α/α' with hexagonal close-packed (hcp) crystal structure possesses a smaller number of slip systems than bcc β . Additionally, more V element in α' rises solid strengthening effect and blocks the dislocation movement, therefore a greater force is required and less deformation occurs when fracture happens. The samples heat-treated at 800°C and 850°C for 4 hours and cooled in air contain the most β and the finest lamellar α , and as expected they exhibit the best ductility and acceptable ultimate tensile strength values. As a matter of fact, a large volume fraction of β in Ti6Al4V alloy leads to a low tensile strength and good ductility. A smaller size of lamellar $\alpha + \beta$ in annealing-treated samples indicates higher tensile strength according to the Hall-Petch relationship.

As far as the tensile tests results are concerned, as shown in table 2 and relevant charts, the two additional hours of treatment have different effects with respect to the different parameters analyzed. Considering the effects of the investigated heat treatments, the following trends can be evidenced:

- Young's modulus (E) was calculated for all specimens in the range of 400-800 MPa, and for this parameter it can be seen that 2 additional hours at the treatment temperature brings an increase of 10 and 8 GPa, respectively, although, on the other hand, the standard deviation is almost tripled for both cycles. This result is in agreement with literature results, ascribing the lower values of the Young's modulus to the texturing deriving from L-PBF [31]. During solidification, the bcc β phase preferentially grows in the $\langle 100 \rangle$ direction, giving rise to long, columnar prior β grains. The $\langle 100 \rangle$ direction of each of these columnar grains

is thus oriented quasi parallel to the build direction, and the rotation of the grain around this direction is considered to be random, causing the presence of a fiber-like texture. [32]

- Concerning the yield strength (Rp), it can be seen that two hours of additional heat treatment have different effects depending on the temperature. At 800°C increasing from 2 to 4 hours leads to a lowering of the nominal Rp values and also to a higher standard deviation, which becomes almost two times the standard deviation obtained with the 2-hour treatment. For the 835°C treatment, on the other hand, the 4-hour treatment seems to improve over the 2-hour treatment, but only for the nominal value of Rp; in fact, the standard deviation of the data, increasing from 2 to 4 hours treatment time, leads to a 4-times increase.
- The same trend occurs for the Ultimate tensile strength (Rm) values: for the 800°C treatment, the additional two hours are detrimental, while for the 835°C treatment the additional two hours lead to a moderate increase. Again, the standard deviation, when passing from 2 to 4 hours, increases significantly, regardless of temperature.
- For the elongation values, on the other hand, the trend seems to affect both the nominal values and the dispersion of the data. At 800°C the 4-hour treatment confers 2 percentage points more to the nominal elongation value, increasing the standard deviation by about 3 times. For the treatment at 835°C, on the other hand, the 4-hour treatment is about 2 percentage points worse than the 2-hour treatment, but a very low standard deviation can be seen, about one-third that of the shorter treatment; this indicates the achievement of higher homogeneity in the sample.

Micrographic examination

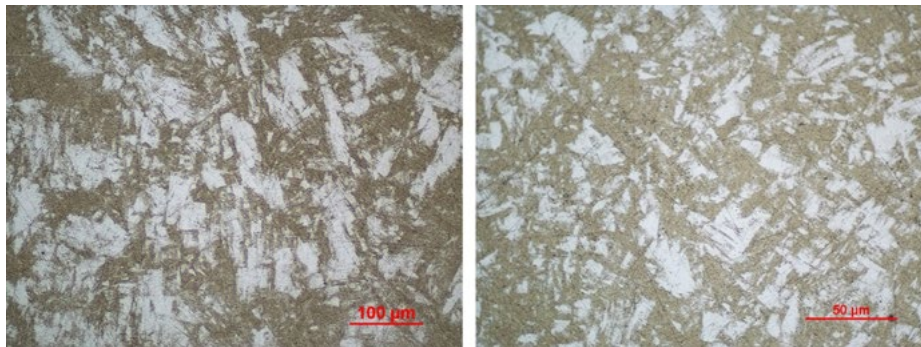


Fig.1 - OM micrographs of Ti-6Al-4V following C1 single annealing thermal cycle at 800°C x 2h, magnification 200x and 500x.

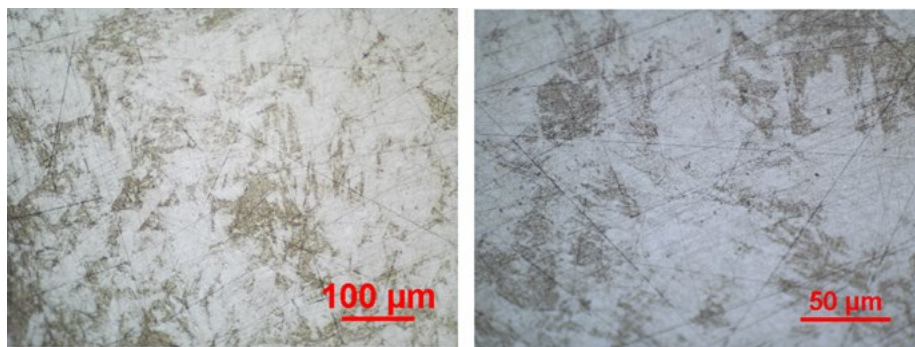


Fig.2 - OM micrographs of Ti-6Al-4V following C3 single annealing thermal cycle at 800°C x 4h, magnification 200x and 500x.

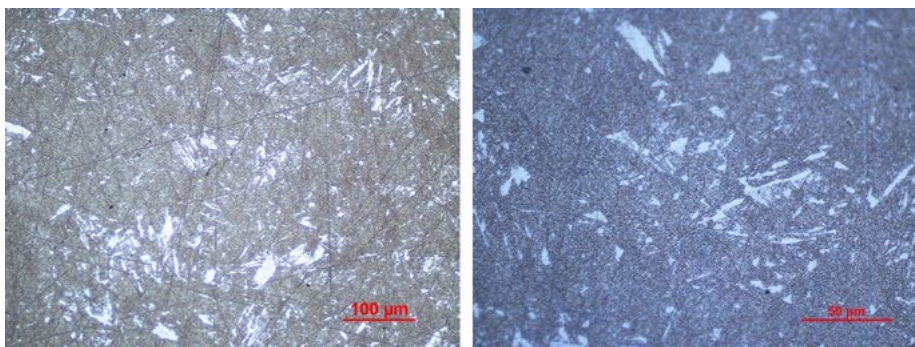


Fig.3 - OM micrographs of Ti-6Al-4V following C2 single annealing thermal cycle at 835°C x 2h, magnification 200x and 500x.

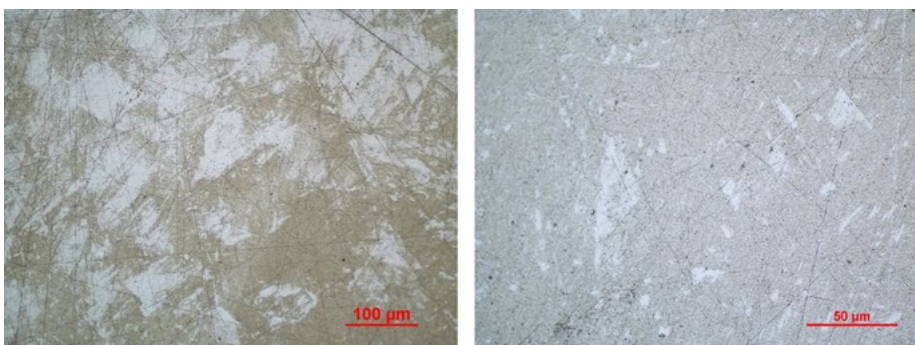


Fig.4 - OM micrographs of Ti-6Al-4V following C4 single annealing thermal cycle at 835°C x 4h, magnification 200x and 500x.

In the figures, a comparison in a different magnification of various individual annealing cycles conducted on the samples is presented.

The figures clearly depict that the resulting microstructure in all heat-treated samples consists primarily of an α acicular phase. In these microstructures, the fine α prime needles, generated due to a sequence of rapid heating and cooling cycles typical of the LPBF process, are still visible, despite the heat treatment. This phenomenon of martensitic structure creation occurs because the high cooling rates used in LPBF processing deplete the vanadium content present in the material matrix; this element is a strong β stabilizer for the titanium alloys, and its absence allows for the formation of α prime.

When examining the cycle carried out at 800°C for 2 hours and 4 hours, notable discrepancies emerge, particularly in terms of the extent of transformation of the prior alpha prime phase. Specifically, the transformation is more pronounced in the latter case, where the samples were subjected to an additional two-hour annealing process at 800°C. Furthermore, this prolonged treatment results in a more homogeneous structure, with the alpha phase being uniformly arranged in more coarsened grains.

Similar observations can be made for the treatment performed at 835°C, although there are not such marked differences. This can be attributed to the fact that the higher treatment temperature already promotes the transformation process during the first two hours, thereby diminishing the influence of the treatment time parameter compared to the cycle performed at a lower temperature.

XRD Analysis

Figure 5 shows XRD data collected from the specimens exposed to the various heat treatments (C1-C4). The full angular range (a) is shown together with a limited one (b). The main hcp phase is indexed according to space group P63/mmc [33]. The positions of observed reflections assigned to body-centered cubic β -phase (space group Im-3m [34]) are indicated, and the main one is better pictured in the limited angular region shown in Figure 5b. Distinguishing between alpha and alpha prime phases is challenging as both of them exhibit the same hexagonal structure [35]. However, comparative evaluations based on the ratio between the cell parameters c and a can give

some indications on the presence of martensite. Hence, this parameter was determined using the angular positions of the hcp reflections and the results are shown in Figure 5c. Data for the as-received powder was also included in this plot [30].

The shift of the peak suggests the absorption of vanadium by the cell, leading to an enlargement of the cell. One answer could be that, in the face of a massive transformation of the alpha prime phase, vanadium has undergone diffusion phenomena within the cell.

The c/a ratio is higher for the annealed samples with respect to the powder [30]. An important increase in the ratio is observed following prolonged annealing at 835 °C, indicating a more important heat-induced transformation from alpha to alpha prime (microstructural modification).

The temperature of 835°C is far from both that of beta transus (996°C) and at that of solubilization (about 960°C), so we cannot speak of a phase transformation, but of a solid-state transition from alpha prime to alpha

In order to better understand the transformations occurring during the heat treatment, it is useful to identify some relevant temperature ranges, as suggested by Ter Haar et al. [36]. In this paper, the understanding of the mechanism of grain morphology transformation in the solid solution temperature region (SSTR) is linked to three main regions: heat treatments conducted in the low-, medium- and high-SSTR. While the low and medium are useful to determine the annealing strategy for decomposing α' into a stable dual phase lamellar $\alpha + \beta$ microstructure, the high-SSTR is used when describing the fragmentation and globularisation to achieve more equiaxed primary α -grains, which is outside of the scope of this paper.

A slightly modified version of their graph is shown in Figure 6, where the temperatures used in this study are indicated by arrows, and help understanding the criteria used to select the heat treatment strategy used during this research.

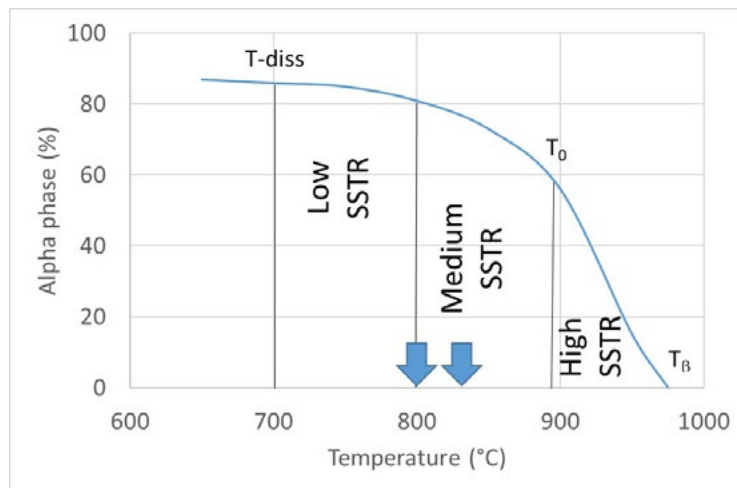


Fig.5 - Schematic of temperature regions and key temperatures in the SSTR (Solid Solution Temperature Region) vs estimated alpha phase fraction [adapted from 36].

Within this solid solution in the aforementioned study, the α -phase served as the solute, while the β -phase acted as the matrix. The SSTR, in this context, encompassed the temperature range between the dissolution temperature (T_{diss}) and the β -transus temperature (T_{β}). The dissolution temperature was identified as the point at which the β -phase began to exponentially increase in volume percentage as a result of the dissolving of the α -phase into the β -phase. For the purposes of the study of Ter Haar et Al. [36], the dissolution temperature was determined to be 705 °C.

Furthermore, the SSTR was divided into three distinct regions: low-, medium-, and high-SSTR. The low- and

medium-SSTRs were situated below a critical temperature (T_0), while the high-SSTR lay above T_0 . The critical temperature denoted the temperature above which α' phase formation occurs during rapid cooling (water–WQ or air cooling–AC). Based on thermodynamic data T_0 was calculated to be 893 °C and 872 °C, respectively. The low- and medium-SSTR regions were separated by a temperature range recognized by various researchers as the region where α' decomposes into α upon heating, yielding favorable tensile results.

The heat treatments used in this study were designed to emphasize the impacts of dwell temperature and dwell time.

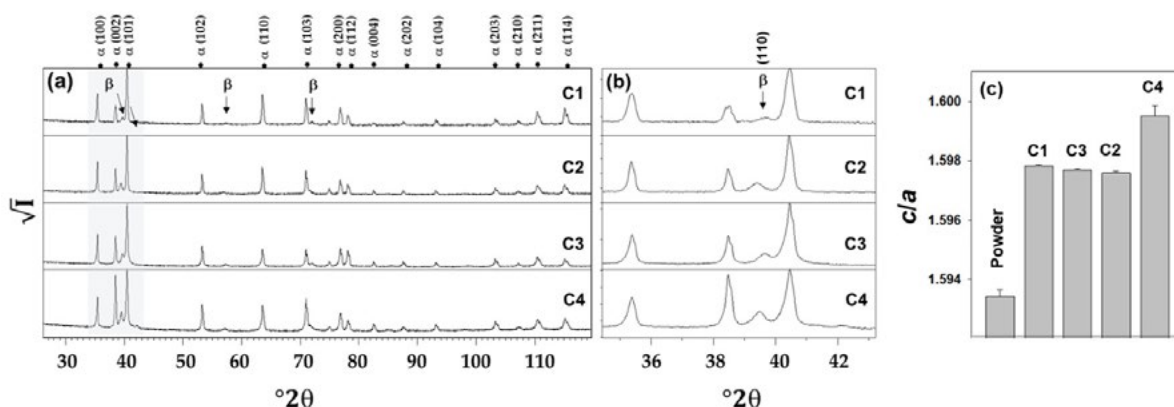


Fig.6 - XRD data collected from annealed samples: 800 °C for 2h (C1); 800 °C for 4h (C2); 835 °C for 2 h (C3); 835 °C for 4h (C4). The full angular range is shown in (a) whereas a limited one is shown in (b), the latter aimed at better visualize the strongest reflection of the β -phase. In (c), the c/a ratio of the hexagonal phase (α/α') in the annealed samples is shown together with data for the as-received powder (previously published [30]).

During the creation of the specimen, the cooling time is so fast that the resulting structure can only be the alpha prime, which is a metastable solid solution composed of alpha phase and beta phase. The lattice structure of the alpha prime is HCP, but due to the presence of the beta phase elements (i.e., vanadium), the HPC cell packing factor of the alpha prime is very low.

The low packing factor indicates that the structure will have a narrow and wide shape.

The moment I go to perform annealing treatments between the transformation start temperature (about 760°C) and the beta transus temperature (about 996°), the alpha prime starts to separate into alpha a and beta. As the kinetics of the transition can be assumed that the vanadium begins to leave the HCP cell, which thus become alpha phase (with

a long and narrow HCP cell) and go to the grain boundary , with a BCC cell.

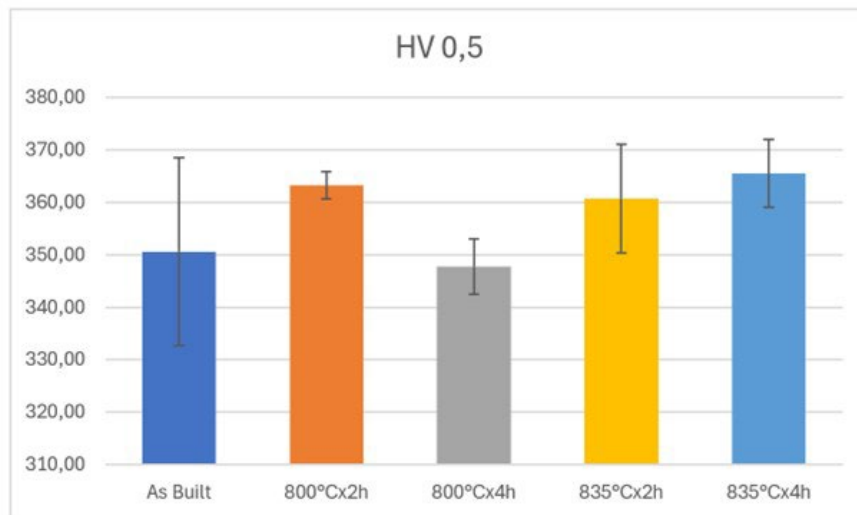
800° is a temperature that does not allow one to see much improvement from the point of view of beta phase transformation between 2 and 4 hours, but only an enlargement of the grain. This would also explain the improvement in elastic modulus.

835, on the other hand, is a temperature at which the improvement from 2 to 4 hours can be appreciated, because, as can be seen from the c/a graph, the C4 treatment leads to a noticeable conversion of the alpha prime phase, with a noticeable increase in the beta phase.

Micro hardness

Tab.3 - Micro hardness test result and graphic.

Microhardness test results			
CYCLE	HV 0,5	MAX	Min
As Built	350,6 ± 17,9	379,6	327,9
C1 (800°Cx2h)	363,22 ± 2,65	367,1	361,3
C2 (800°Cx4h)	360,68 ± 10,63	373,3	336,9
C3 (835°Cx2h)	347,76 ± 5,32	355	342,6
C4 (835°Cx4h)	365,5 ± 6,52	379,7	355,5



The results of the microhardness analyses follow the trend of the tensile tests for the parameters Rp and Rm. For the treatment carried out at 800°C, the best dwell time is the 2-hour dwell time, as the 4-hour dwell time both depresses the nominal hardness value and increases the

inhomogeneity of the data by about 5 times. For the heat treatment carried out at 835°C, on the other hand, two more hours of dwell time is ameliorative in that it increases the hardness by about 5 percent, going on to slightly increase the standard deviation of the datum.

CONCLUSION

This work aims to analyze the different effects of residual stress reduction treatments performed on Gr. 5 titanium specimens obtained by additive manufacturing. Specifically, the main objective of the research is to investigate the influence of the heat treatment time on the material properties, starting from the results obtained from the previous study [30], where two temperature ranges (800°C x 2h and 835°C x 2h, respectively) had been identified and had provided encouraging results both in terms of mechanical properties and homogeneity of the values obtained within the same job.

With this premise in mind, the heat treatment time was then extended, leaving all other test conditions unchanged, to a total duration of 4h with the aim of verifying whether this strategy could allow further improved results over those previously obtained.

The main purpose of the stress relief treatments performed on Ti 6Al 4V parts obtained by additive manufacturing is to maximize the strength response of the material but also to obtain a homogeneous result on all the samples grown in different positions of the printing area.

Looking at the results obtained by increasing the dwell time to 4h total, it can be observed that:

- Comparing the results of the two different dwell times of 2h and 4h at T 800°C, respectively, it can be seen that the results of the mechanical properties are not improved at all by increasing the dwell time in the furnace; both the unit yield strength and the unit tensile strength are lower, and the standard deviation is also worsened. This result is also confirmed by the microhardness tests, where the distribution of results is extremely scattered
- Conversely, for the samples treated at 835 °C, prolonging the treatment time to 4h marks an increase in mechanical properties around 3-4%, although the standard deviation of the results is worsened, as is the elongation at break. The result of the tensile tests is again confirmed by the microhardness trend, which in this case is higher for the longer duration treatment

Micrographic examination revealed that all heat-treated samples exhibited a predominantly α acicular phase. The presence of α prime needles, characteristic of the LPBF

process, was still observed despite the heat treatment. The transformation of the alpha prime phase was more pronounced with the 4-hour treatment at 800°C, leading to a more homogeneous structure. Similar observations were made for the treatment at 835°C, although the differences were less noticeable due to the higher treatment temperature.

XRD analysis confirmed the presence of the hcp phase and indicated the absorption of vanadium by the cell, resulting in an enlargement of the cell. The c/a ratio, which provides insights into the presence of martensite, increased with prolonged annealing at 835°C, indicating a significant heat-induced transformation from alpha to alpha prime.

It has been repeatedly discussed in the literature how the optimal treatment parameters for Ti 6Al 4V alloy must exhibit a balance of process temperature and thermal cycle duration parameters. This paper, together with the previous paper by some of the authors, basically show two main results:

- It is necessary to choose a treatment temperature > 780°C (see fig 6) in order to achieve an initial alpha prime transformation in industrial-compatible cycles. The best results in terms of general mechanical properties and, above all, homogeneity of results was obtained with the samples treated @835°C, although those treated at @800°C, i.e. in the low range of the medium SSTR, had already appreciable properties although slightly more dispersed
- Conversely, the treatment time turned out to be a variable that was not so significant, and indeed, in the case of the treatment @800°C for 4h, the results turned out to be worse than the results obtained with shorter times.

An interesting result obtained from the present study by analyzing the data from the treatments with a duration of 4h is the significant increase recorded in the elastic modulus of the material, which is almost 10% higher than the values previously found on this alloy. A scientific explanation for this result, possibly related to texturing, cannot be given at present, and it will be further investigated and deepened in the future by generating samples with different orientations.

In conclusion, this study contributes to the understanding of the effects of different heat treatment strategies on the alloy and provides valuable insights for optimizing the post-process heat treatment of additively manufactured titanium components.

REFERENCES

- [1] Mercelis, P.; Kruth, J. Residual stresses in selective laser sintering and selective laser melting. *Rapid Prototyp. J.* 2006, 12, 254–265.
- [2] Bartolomeu, F.; Gasik, M.; Silva, F.S.; Miranda, G. Mechanical Properties of Ti6Al4V Fabricated by Laser Powder Bed Fusion: A Review Focused on the Processing and Microstructural Parameters Influence on the Final Properties. *Metals* 2022, 12, 986.
- [3] Yang, J.; Yu, H.; Yin, J.; Gao, M.; Wang, Z.; Zeng, X. Formation and control of martensite in Ti-6Al-4V alloy produced by selective laser melting. *Mater. Des.* 2016, 108, 308–318.
- [4] Antonysamy, A.A.; Meyer, J.; Prangnell, P.B. Effect of build geometry on the β -grain structure and texture in additive manufacture of Ti6Al4V by selective electron beam melting. *Mater. Char.* 2013, 84, 153–168. [CrossRef]
- [5] Yassine, L.; Connétable, D.; Hugues, J.; Hermantier, P.; Barriobero-Vila, P.; Dehmas, M. Microstructural evolution during post heat treatment of the Ti-6Al-4V alloy manufactured by laser powder bed fusion. *J. Mater. Res. Technol.* 2023, 23, 1980–1994.
- [6] Etesami, S.A.; Fotovvati, B.; Asadi, E. Heat treatment of Ti-6Al-4V alloy manufactured by laser-based powder-bed fusion: Process, microstructures, and mechanical properties correlations. *J. All. Comp.* 2022, 895, 162618. [CrossRef]
- [7] Xu, W.; Lui, E.W.; Pateras, A.; Qian, M.; Brandt, M. In Situ Tailoring Microstructure in Additively Manufactured Ti-6Al-4V for Superior Mechanical Performance. *Acta Mater.* 2017, 125, 390–400. [CrossRef]
- [8] Cao, S.; Zou, Y.; Lim, C.V.S.; Wu, X. Review of Laser Powder Bed Fusion (LPBF) Fabricated Ti-6Al-4V: Process, Post-Process Treatment, Microstructure, and Property. *Adv. Manuf.* 2021, 2, 20. [CrossRef]
- [9] Ter Haar, G.M.; Becker, T.H. The influence of microstructural texture and prior beta grain recrystallisation on the deformation behaviour of laser powder bed fusion produced Ti-6Al-4V. *Mater. Sci. Eng. A* 2021, 814, 141185. [CrossRef]
- [10] Cao, S.; Hu, Q.; Huang, A.; Chen, Z.; Sun, M.; Zhang, J.; Fu, C.; Jia, Q.; Lim, C.V.S.; Boyer, R.R.; et al. Static coarsening behavior of lamellar microstructure in selective laser melted Ti-6Al-4V. *J. Mater. Sci. Technol.* 2019, 35, 1578–1586. [CrossRef]
- [11] Yan, X.; Chen, C.; Huang, C.; Bolot, R.; Kuang, M.; Ma, W.; Coddet, C.; Liao, H.; Liu, M. Effect of heat treatment on the phase transformation and mechanical properties of Ti6Al4V fabricated by selective laser melting. *J. Alloys Compd.* 2018, 764, 1056–1071. [CrossRef]
- [12] Khorasani, A.M.; Gibson, I.; Goldberg, M.; Littlefair, G. On the role of different annealing heat treatments on mechanical properties and microstructure of selective laser melted and conventional wrought Ti-6Al-4V. *Rapid Prototyp. J.* 2017, 23, 295–304. [CrossRef]
- [13] Ghods, S.; Schur, R.; Schleusener, R.; Montelione, A.; Pahuja, R.; Wisdom, C.; Arola, D.; Ramulu, M. Contributions of Intra-Build Design Parameters to Mechanical Properties in Electron Beam Additive Manufacturing of Ti6Al4V. *Mater. Today Commun.* 2022, 30, 103190. [CrossRef]
- [14] Charles, A.; Elkaseer, A.; Thijs, L.; Scholz, S. Effect of build platform location and part orientation on dimensional accuracy of down-facing surfaces in LPBF. In *Proceedings of the Conference: World Congress on Micro and Nano Manufacturing 2021, Bombay, Mumbai, India, 21–23 September 2021.*
- [15] Yang, Z.; Yang, M.; Sisson, R.; Li, Y.; Liang, J. A machine-learning model to predict tensile properties of Ti6Al4V parts prepared by laser powder bed fusion with hot isostatic pressing. *Mater. Today Commun.* 2022, 33, 104205.
- [16] Etefagh, A.H.; Zeng, C.; Guo, S.; Raush, J. Corrosion behavior of additively manufactured Ti-6Al-4V parts and the effect of post annealing. *Addit. Manuf.* 2019, 28, 252–258
- [17] Qiu, C.; Adkins, N.J.E.; Attallah, M.M. Microstructure and Tensile Properties of Selectively Laser-Melted and of HIPed Laser Melted Ti-6Al-4V. *Mater. Sci. Eng. A* 2013, 578, 230–239.
- [18] Ducato, A.; Fratini, L.; La Cascia, M.; Mazzola, G. An Automated Visual Inspection System for the Classification of the Phases of Ti-6Al-4V Titanium Alloy. In *Computer Analysis of Images and Patterns; CAIP 2013, Part II, LNCS 8048; Wilson, R., Hancock, E., Bors, A., Smith, W., Eds.; Springer: Berlin/Heidelberg, Germany, 2013; pp. 362–369.*
- [19] Vilaro, T.; Colin, C.; Bartout, J.D. As-Fabricated and Heat-Treated Microstructures of the Ti-6Al-4V Alloy Processed by Selective Laser Melting. *Metall. Mater. Trans.* 2011, 42, 3190–3199.
- [20] Simonelli, M.; Tse, Y.Y.; Tuck, C. Effect of the build orientation on the mechanical properties and fracture modes of SLM Ti-6Al-4V. *Mater. Sci. Eng. A* 2014, 616, 1–11.
- [21] Longhitano, G.A.; Larosa, M.A.; Jardini, A.L.; Zavaglia, C.A.D.C.; Ierardi, M.C.F. Correlation between Microstructures and Mechanical Properties under Tensile and Compression Tests of Heat-Treated Ti-6Al-4V ELI Alloy Produced by Additive Manufacturing for Biomedical Applications. *J. Mater. Process. Technol.* 2018, 252, 202–210.
- [22] Vrancken, B.; Thijs, L.; Kruth, J.-P.; Van Humbeeck, J. Heat Treatment of Ti6Al4V Produced by Selective Laser Melting: Microstructure and Mechanical Properties. *J. Alloys Compd.* 2012, 541, 177–185.

- [23] Brot, G.; Koutiri, I.; Bonnand, V.; Favier, V.; Dupuy, C.; Ranc, N.; Aïmedieu, P.; Lefebvre, F.; Hauteville, R. Microstructure and Defect Sensitivities of LPBF Manufactured Ti-6Al-4V in Accelerated 20 KHz Fatigue Response. SSRN J. 2022
- [24] Chao, Q.; Hodgson, P.; Beladi, H. Thermal stability of an ultrafine grained Ti-6Al-4V alloy during post-deformation annealing. *Mat. Sci. Eng. A* 2017, 694, 13–23.
- [25] Sun, Y.; Aindow, M.; Hebert, R.J. Comparison of Virgin Ti-6Al-4V Powders for Additive Manufacturing. *Addit. Manuf.* 2018, 21, 544–555.
- [26] Levinger, B.W. Lattice parameters of beta titanium at room temperature sample: At $T = 298\text{K}$, known as the beta phase. *J. Met.* 1953, 5, 195.
- [27] Wysocki, B.; Maj, P.; Sitek, R.; Buhagiar, J.; Kurzydłowski, K.J.; Świąszkowski, W.; Świąszkowski, W. Laser and electron beam additive manufacturing methods of fabricating titanium bone implants. *Appl. Sci.* 2017, 7, 657.
- [28] Oh, J.-M.; Lee, B.-G.; Cho, S.-W.; Lee, S.-W.; Choi, G.-S.; Lim, J.-W. Oxygen effects on the mechanical properties and lattice strain of Ti and Ti-6Al-4V. *Met. Mater. Int.* 2011, 17, 733–736.
- [29] Cho, J. Characterization of the α_0 -Martensite Phase and Its Decomposition in Ti-6Al-4V Additively Manufactured by Selective Laser Melting; RMIT University: Melbourne, Australia, 2018
- [30] Gaiani, S.; Ferrari, E.; Gozzi, M.; Di Giovanni, M.T.; Lassinantti Gualtieri, M.; Colombini, E.; Veronesi, P. Impact of Post-Process Heat Treatments Performed on Ti6Al4V Titanium Alloy Specimens Obtained Using LPBF Technology. *Technologies* 2023, 11, 100. <https://doi.org/10.3390/technologies1104100>
- [31] *Journal of Alloys and Compounds*, 2012. 541(0): p. 177-185. doi: 10.1016/j.jallcom.2012.07.0
- [32] L. Thijs, F. Verhaeghe, T. Craeghs, J. Van Humbeeck and J. P. Kruth. A study of the micro structural evolution during selective laser melting of Ti-6Al-4V. *Acta Mater.* 58 (2010) 3303-3312
- [33] T. Novoselova, S. Malinov, W. Sha, A. Zhecheva, High-temperature synchrotron X-ray diffraction study of phases in a gamma Ti Al alloy, *Materials Science and Engineering A*, 2004, 371, 103-112
- [34] Levinger, B.W. Lattice parameters of beta titanium at room temperature sample: At $T = 298\text{K}$, known as the beta phase. *J. Met.* 1953, 5, 195
- [35] Wysocki, B.; Maj, P.; Sitek, R.; Buhagiar, J.; Kurzydłowski, K.J.; Świąszkowski, W.; Świąszkowski, W. Laser and electron beam additive manufacturing methods of fabricating titanium bone implants. *Appl. Sci.* 2017, 7, 657.
- [36] Ter Haar, G. M., & Becker, T. H. (2018). Selective laser melting produced Ti-6Al-4V: Post-process heat treatments to achieve superior tensile properties. *Materials*, 11(1). <https://doi.org/10.3390/ma1101014>

TORNA ALL'INDICE >